

FAR-FIELD FAN NOISE ESTIMATION WITH THE APPLICATION OF 3D AEROACOUSTIC CALCULATION

Rossikhin A.A., Khaletskiy Y.D., Mileschin V.I.
Central Institute of Aviation Motors (CIAM), Moscow

Keywords: *fan, aeroacoustics,*

Abstract

In the work are presented the effort of aircraft flyover noise estimations with the usage of data, obtained in the 3 dimensional unsteady calculation of tone noise of high bypass ratio fan of turbofan designed for a medium range, single-aisle civil aircraft with two engines. Calculation was performed using CIAM 3DAS (3 Dimensional Acoustics Solver) in-house solver created for simulation of turbomachinery tone noise.

1 Introduction

An important problem of modern turbo-engine industry is the problem of turbomachine noise reduction. It arisen due to continuous stringency of noise regulations. The only way to remain in forefront is based on the comprehensive investigation and consequential suppression of noise generation mechanisms in turbomachines.

A numerical method for turbomachinery noise generation and propagation calculation was developed in CIAM in the beginning of 2000th. The method is implemented in the 3DAS [1,2] (3 Dimensional Acoustics Solver) CIAM in-house aeroacoustic solver. The 3DAS solver can be used for tone noise calculation of different types of turbomachines. It was applied for calculation of tone noise of counter-rotating open rotors [1] and ducted counter-rotating fans [3], with quite promising results. Satisfactory results were obtained in the calculations of tone noise of ducted classical single-rotated fans for

approach [4], cutback, and sideline [5] operational conditions. Also the solver was used for the calculation of acoustic characteristics of last stages of low pressure turbines [2].

In the cases of ducted fans all calculations of tone noise were performed for the fan models mounted in the test rig C3-A. However for optimization of fan acoustic characteristics it is more important to be able to predict contribution of fan noise to an aircraft flyover noise. This work is devoted to aircraft flyover noise estimations with the usage of data, obtained in the 3D unsteady calculation of the tone noise of a fan of the aircraft turbofan.

The CIAM test rig C3-A was designed for measurement of acoustic characteristics of single rotating and counter-rotating fans [6]. In this test rig the fan model was mounted on the console by its rear part. Also the inlet in most experiments had simple un-flanged form. So the radiation of a fan in the test rig setup may differ from the radiation of the fan mounted in the engine nacelle. The difference between directivity diagrams for different types of inlets and nozzles is also the point of this work.

The initial data for this work is the data for structure of the acoustic pulsations upstream and downstream of the fan, which was obtained in the work presented in the paper [4]. Here we recalculated the noise of the fan using inlet and outlet corresponding to the case of the fan mounted in the engine nacelle. Flight effects were also taken into account. Comparison between directivity diagrams for the different

inlets and outlets (for the rig and for the nacelle) was carried out.

Results of the tone noise calculation of the fan under consideration were used for estimation of the flyover noise of the airplane. The results of the estimation were compared with the data, obtained using semiempirical model of fan tone noise.

2 3DAS Solver

In the last two decades significant efforts were applied for the development of fast and robust methods for turbomachinery tone and broadband noise calculations [7], [8], [9]. In CIAM the 3DAS solver was designed [1] for the calculations of tone noise generation by a turbomachine, tone noise propagation through the duct of a turbomachine and tone noise radiation from the vicinity of a turbomachine to the far field.

The method implemented in the solver is based on the decomposition of the unsteady viscous 3D flow into two parts - inhomogeneous viscous 3D steady flow field and 3D unsteady inviscid disturbances. The input data for the solver is a steady mean flow field in the computational domain and a body-fitted computational grid. For turbomachinery tone noise applications the steady mean flow field in the blade rows must be calculated using a Reynolds-Averaged Navier–Stokes (RANS) finite volume steady equations and "mixing-plane" interfaces between blade rows. Calculation of unsteady inviscid equations for disturbances (linear or nonlinear dependent on the problem) over the mean steady flow field is performed in the reference frame rotating with the blade row. Interaction between blade rows is provided by special interfaces which preserves continuity of flow parameters through the boundary.

The equations in our method are solved using numerical methods of computational aeroacoustics. For spatial approximation we use the fourth order DRP (Dispersion Relation Preserving) scheme [10], generalized to the finite volume method [1]. For time derivative approximation second order, four stages Runge-Kutta LDDRK (Low Dissipation and Dispersion

Runge-Kutta) scheme [11] is used. To suppress high wave number spurious waves, artificial selective damping is used, based on the fourth-order central filtering coefficients of O. Vasilyev [12]. 3DAS solver admits calculations either in time domain or in frequency domain for specified set of harmonics [2].

In general 3DAS solver allows performing calculation of tone noise generation and propagation in one computation. However to simplify a problem and reduce calculation time we use hybrid approach. In this approach (see for example [7]) the problem of turbomachinery tone noise generation is divided into two parts: inter-row (rotor-stator or rotor-rotor) interaction problem and problem of noise propagation through the duct. The results of the inter-row interaction calculation are used as input data for the propagation calculation.

The matching between the problems of interaction and propagation is organized [2], by decomposition of the perturbation field on the prescribed cross-section of computational domain on acoustic modes (eigenmodes) in the coaxial cylindrical duct. Outgoing acoustic modes extracted from the solution of the first problem are used as input data for the second one.

The problem of noise propagation calculation can be simplified if the duct is axisymmetric (which is the usual case for test rigs). In this case, the solution can be decomposed on circumferential modes (harmonic functions of time and circumferential angle), and calculation can be performed independently for each mode on two-dimensional domain corresponding to longitudinal section of initial three-dimensional geometry. Calculation is performed in frequency domain. In many cases the solutions can be described by quite small number of circumferential modes, so the reduction of 3D problem to the set of 2D problems can lead to the saving of computational resources. In conjunction with this method we use the method, based on the gradient terms suppression (GTS) in the linearized Euler equations [13] to provide their stability in the shear layer of the jet.

The method based on the Ffowcs-Williams and Hawkins equation with a penetrable data (integration) surface [14] was implemented in the solver to predict tone noise in the far field, using results of the calculations in the near field.

3 Input data

The essence of the paper is the calculation of tone noise of a high bypass ratio (>8) fan mounted in the engine nacelle taking into account flight effects. We considered a fan working at subsonic approach conditions. As initial data for our calculations we use the results of rotor-stator interaction calculations for this fan, obtained during the far field tone noise calculations for the fan mounted in the test rig [4].

The fan under consideration in the rig setup is a 700 mm wide chord fan model with swept stator vanes, designed for an advanced turbofan of civil aircraft. The description of the model can be found in [4] and references therein. It has 18 blades in the rotor and 41 vanes in the stator. The model contains 3 booster stages. The number of input guide vanes of the booster is 71. Also it contains 8 struts in the bypass duct right after the stator and 8 supporting struts in the exit of the bypass duct. The scheme of a fan model in the test rig setup can be seen in the fig. 1. Fig. 2 shows rotor and stator of the fan.

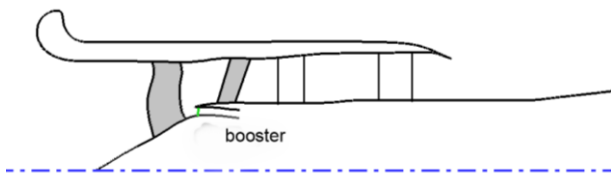


Fig. 1. Generic scheme of a fan model

The approach operational conditions correspond to relative shaft speed, $N = 53.9\%$.

The test campaigns for the fans in the rig setup were performed, as it was mentioned earlier, in the C-3A test facility [6]. It is designed for acoustic, aerodynamic, and mechanical investigations of counter rotating and conventional fan models. In this facility it is possible to measure fan noise at forward and

rear hemisphere simultaneously. The measurement system includes 24 microphones. The fig. 3 presents a photo of a fan model without turbulence control screen (TCS).



Fig. 2. Photos of the tested fan model rotor and stator

In the present work we intend to study acoustic characteristics of the fan mounted in the engine nacelles. In order to obtain these results we have to scale the modal analysis data for rig size to the engine size. Then we have to calculate noise propagation through the inlet and the nozzle of the engine nacelle. In general an inlet of an engine nacelle has complex 3 dimensional structure. In the paper, which is our first approach to the problem, we are bounded ourselves by the axisymmetric form of the nacelle. This simplification greatly accelerates the calculations and nevertheless allows investigating the effect on radiation caused by the geometry of the inlet and the structure of flow field.

The nacelle, used in the calculations is shown in the fig. 4. It is quite typical for the modern engines. The parameters of the bypass duct (pressure ratio, mass flow rate,

temperature) were determined using parameters of the fan model. The parameters of the core duct were determined partly from fan parameters (mass flow rate), partly from data about jet parameters found in the literature (pressure ratio, temperature).



Fig. 3. C-3A CIAM acoustic test facility

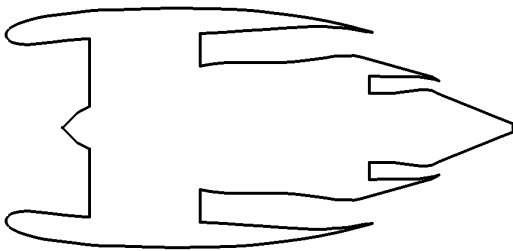


Fig. 4. Scheme of the nacelle

To compare separately the influence of the geometry and the influence of external flow field it seems reasonable to perform calculation of noise propagation through the engine nacelle for two cases - the case of a nacelle in static conditions (no flow) and the case of a nacelle in flight conditions. Also as a reference we have to show the computational process for the noise propagation through the rig inlet and nozzle.

4 Calculation of rotor-stator and rotor-guide vanes interactions

The goal of our calculation was to obtain first three cut on harmonics of fan noise (in our case second third and fourth harmonics of blade-passing-frequency - BPF). As a method of calculation we chose one in the frequency domain. A simplified geometrical model of the fan, which contained only rotor, stator in the

bypass duct and inflow guide vanes (IGV) of the booster was used. We neglected the interaction of noise, propagating through bypass duct with the struts and interaction between rotor and struts. Also we neglected tip clearance, because in our case it is quite small relative to the diameter of the fan ($<10^{-3}$).

In order to further simplify the calculations we divided our problem onto two separate problems, - problem of interaction between rotor and stator and problem of interaction between rotor and IGV. In the last case we considered only propagation in the forward hemisphere.

The first stage of the simulation was the computation of mean steady flow fields in approach operational conditions using RANS equations, the semi-empirical model of turbulence, and "mixing-plane" interfaces between blade rows. It was performed with one of the CIAM in-house aerodynamic solvers "3D-IMP_MULTI" [1]. The computational domain included rotor stator and booster.

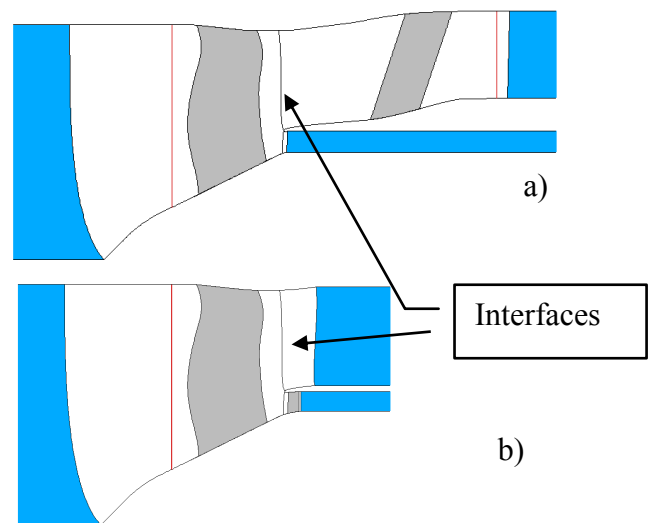


Fig. 5. Schemes of the computational domains. a) rotor-stator interaction; b) rotor - IGV interaction

The computational grid for unsteady simulations was derived from the grid for the steady flow field calculations. For the problem of rotor-stator interaction calculation it included domain, containing rotor blade, domain containing stator vane and domain, containing entrance of the booster. The scheme of

computational domain is presented in the fig. 5a. The computational domain also contains buffer zones to prevent unphysical reflections (partially shown in fig. 5 in blue). Total number of cells is approximately 3 million.

For the problem of rotor-IGV interaction calculation computational domain included domain, containing rotor blade, domain containing IGV vane and domain, containing entrance of the bypass duct. The scheme of computational domain is presented in the fig. 5b. Total number of cells is approximately 2 million.

Unsteady field in our method is described by the set of harmonic fields. As though we are solving equations in the reference frames of blade rows, in the grid blocks, rotating with the rotor we are searching for the solution as a set of fields, corresponding to the harmonics of the frequency of stator vanes or IGV vanes passage relative to the rotor – $\omega = 43 \Omega$ or $\omega = 71 \Omega$. Here Ω – is the shaft rotation angular velocity. Analogously for the blocks connected with the stator or IGV we are searching for the solution as the set of BPF harmonics. Analysis, based on the theory of rotor-stator interaction [15] and authors' experience, showed that in order to obtain tone noise in the specified frequency range in our calculations, we can limit them to the harmonics of Ω listed in the Table 1.

Table 1. Set of harmonics

	Harmonics - rotor	Harmonics - Stator and IGV
Rotor-stator	41, 82, 123	18, 36, 54, 72
Rotor-IGV	71, 142	18, 36, 54, 72

More detailed description of the computation of the rotor stator interaction can be found in [4]. The calculation process for the rotor-IGV interaction computation is analogous.

During the final stage of rotor-stator interaction computation, the unsteady flow field quantities data were collected on surfaces in the fan inlet and outlet (are shown in red in fig. 5). On these surfaces we performed mode decomposition [2]. The results of modal analyses as histograms of power levels for cut on circumferential modes are shown in the fig. 6a,b (red bars - rotor-stator interaction, blue

bars - rotor-IGV interaction). For convenience both histograms have the same initial value of PWL axis. In the histograms the number n represents the frequency of circumferential mode through the BPF (which we will denote as F) - $f=nF$, and m- circumferential number.

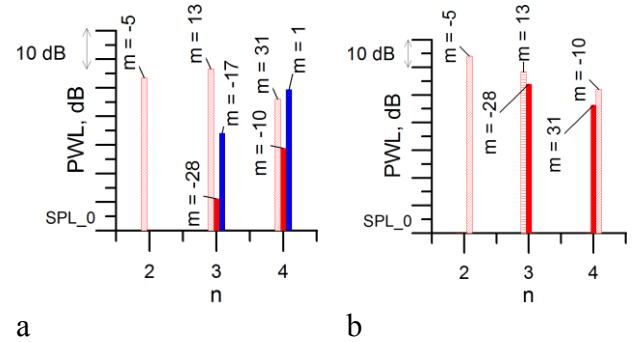


Fig. 6. Results of the modal analysis. a) Forward interaction noise, b) Aft interaction noise

5 Calculation of noise propagation to the far field

Basing on the results of the modal decomposition, we performed the calculations of tone noise propagation through the inlet and the nozzle of the fan. As it was mentioned earlier we considered three cases - noise propagation through the duct of the rig, noise propagation through the duct of the nacelle in the flight conditions and noise propagation through the duct of the nacelle in the static conditions.

For the calculation of the mean steady flow field in all three cases we used CIAM's 3DFS RANS solver [1]. Calculations were performed in inviscid approximation. Computational domains (only the regions of dense grid) and the results of the calculations for the Mach number fields for all three cases are represented in fig. 7a,b,c. Also grids contained buffer zones to prevent unphysical reflections. Though the results for inlet and nozzle of engine nacelle are shown for convenience separately, in the calculation they were the parts of one computational domain. Contrary in the case of the rig they were separate. It is worth noting, that in this paper the computational domain for the rig nozzle was changed in comparison to the work [4] in order to provide the construction of

bigger integration surface, which without intersecting the jet can with guaranty catch all the noise radiated from the nozzle, and solve the

problem of noise leakage through the hole in it (see below).

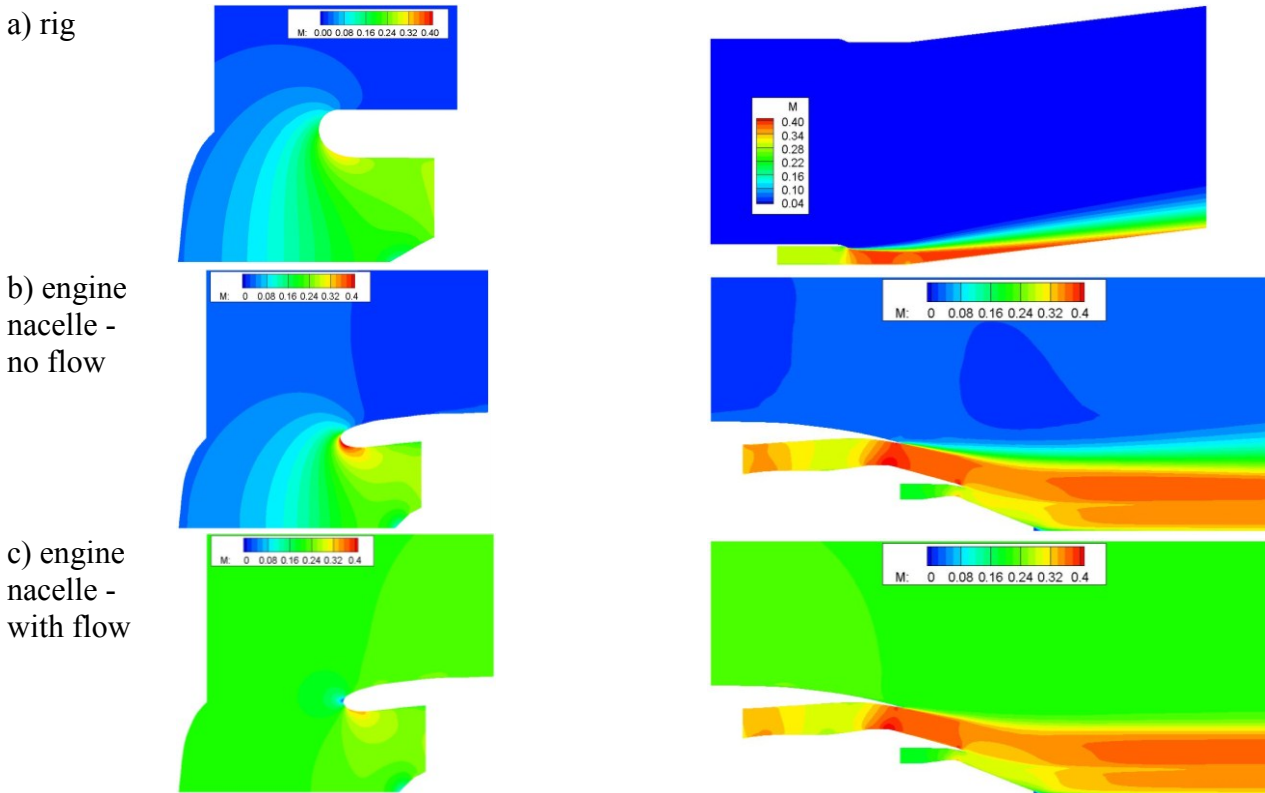


Fig. 7. The results of the calculation for Mach number field in the inlet (left column) and nozzle (right column) in the region of fine grid

Noise propagation in all cases was computed using linearized Euler equations for circumferential modes in the frequency domain for all modes presented in the fig. 6. This is the same approach which was used in the calculations of noise propagation through the inlet in the work [4]. However in the work [4] the calculation of tone noise propagation through the nozzle was performed using unsteady linearized Euler equations in the 3D computational domain. The usage of the more computational power demanding method was inspired by the potential instability of the linearized Euler equations for circumferential mode in the frequency domain in the presence of shear layer. In the current work, in order to accelerate the calculations we used method, based on the suppression of the mean flow gradient terms (GTS) in the linearized Euler equations [13]. This method was used in many

works and its usage was proven to give only small effect on the results of aft noise calculations in most cases. Our investigations showed that in the case of the rig nozzle the effect of the GTS usage is less than 1 dB in most points.

The results of calculation for circumferential mode with $f=3F$, $m=-13$ in the regions of fine grid are showed in the fig. 8a,b,c for all three cases. Black lines in the fig. 8 show positions of the integration surfaces. Comparison between calculations demonstrates that we can expect strong influence of external flow on the directivity of noise.

To compute tone noise radiation in the far field Ffowcs Williams method was used. For the comparison with experiment pressure pulsations were computed for two sets of microphones. In the first set the points are

placed along the arc with $r=4$ m (in the rig scale) and with the center in the point of intersection between the surface containing tips of the leading edges of rotor blades and the axis of shaft rotation. The points had uniform angular distribution within 1-90 degrees with 1 degrees spacing. In the second set pressure pulsations were computed at points placed along the arc with $r=4$ m and the center in the point of intersection between the surface of the

nozzle exit and the axis of shaft rotation. The points had uniform angular distribution within 90-179 degrees with 1 degrees spacing. Also for the comparison with the semi-empirical calculation we performed calculation for the third set of microphones in which microphones are arranged on the half circle at the distance 50 m (in the engine scale) uniformly with 1 degrees spacing.

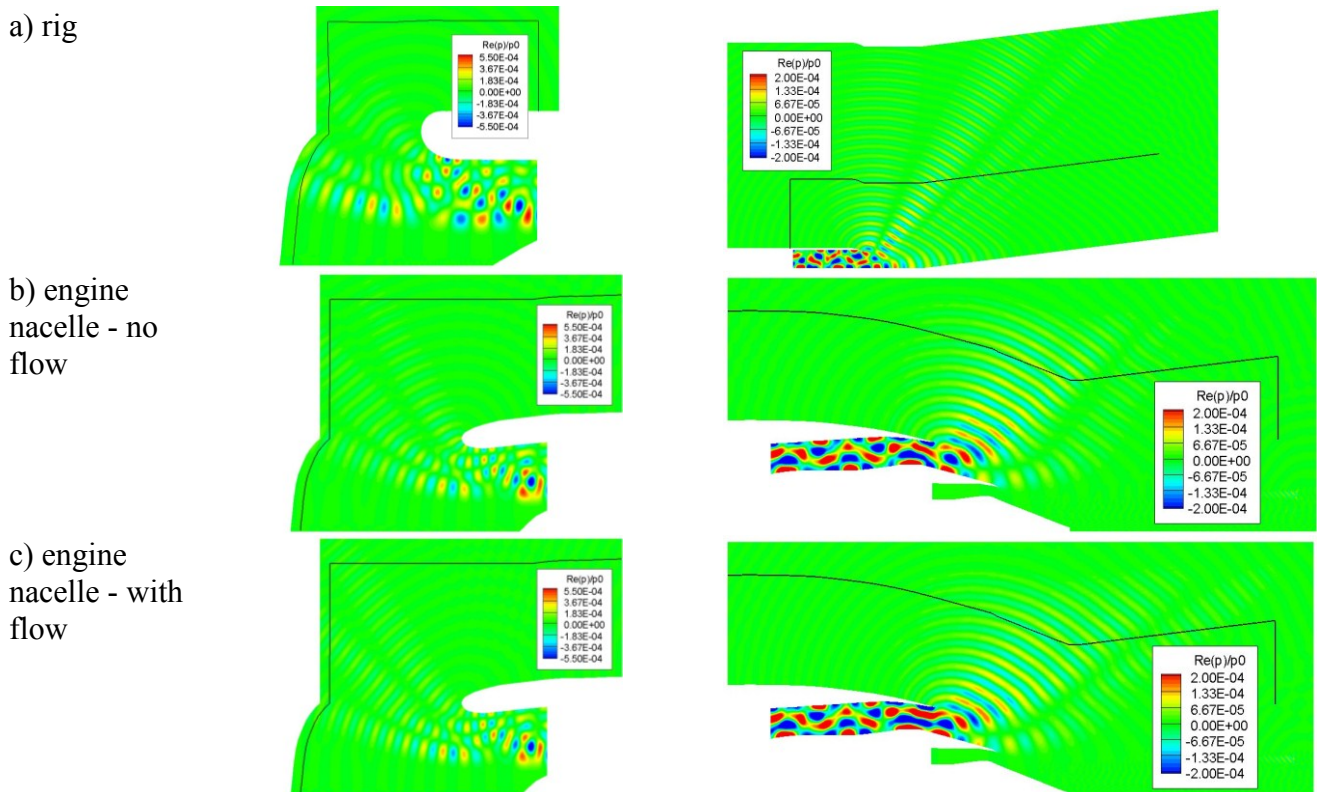


Fig. 8. Real part of static pressure (normalized) pulsations for circumferential mode with $f=3F$, $m=-13$ in inlet (left column) and nozzle (right column)

6 Comparison of the results with the experimental data and semi-empirical calculation

The results, obtained in the previous sections, were compared with the results of the experiment for the fan under consideration in the CIAM test rig C-3A. In the forward hemisphere comparison was performed for 12 microphones placed at the same distance from the fan as in the computation. In the aft hemisphere comparison was performed for 11

microphones. As an initial data for comparison we used narrowband spectra for these microphones obtained in the experiment. The frequency bands of the spectra were equal to 19.5 Hz. On the basis of these spectra were calculated directivity diagrams for the second, third and fourth harmonics of BPF.

First we considered forward hemisphere. In the fig. 9a,b,c (left column) are presented correspondingly the results of calculations in the forward hemisphere for the 2-th, 3-th and 4-th harmonics of BPF. Also we presented the results of experiment for this harmonics.

From the fig. 9 it can be concluded, that the closest correspondence between calculation and experiment for the rig inlet is observed for the second harmonic of BPF. Also calculation and experiment are very close for the fourth harmonic of BPF at small angles (contribution of rotor-IGV interaction). For some positions of microphones the difference between calculation and experiment is less than 2-3 dB. Also we see that the flanged engine inlet suppresses noise for the 2-nd and the 3-rd harmonics.

The results for the aft hemisphere are presented on the fig. 9a,b,c (right column). First of all we should underline, that the results of the rig noise calculations for aft hemisphere are different from those presented in the paper [4]. New form of integration surface allowed us to avoid noise leakage through the hole in the surface, so in some directions the results of calculation changed. Fortunately the change is not significant in the vicinity of most experimental points.

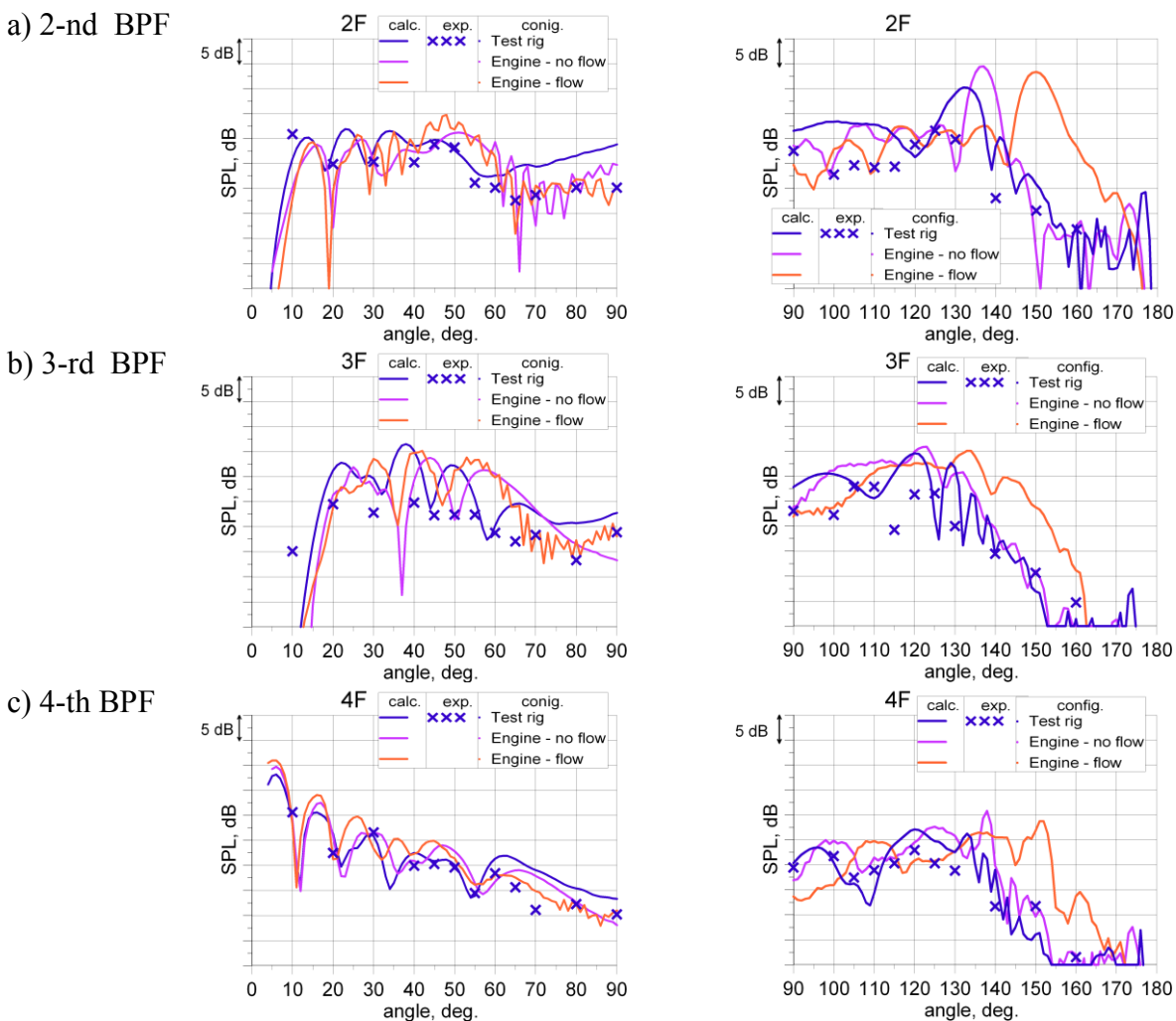


Fig. 9. Comparison between directivity diagrams: left column - forward hemisphere; right column aft hemisphere

Comparison between experiment and calculation showed that aft radiation in the computation is significantly stronger than in the experiment. The maximum of computational curves for the fan lays significantly higher for

all harmonics. Moreover we see significant difference in the directivity diagrams between all three cases, considered in the paper. First of all the positions of maxima in all three cases are different. The difference between the

calculations without flow can be explained by quite different geometries of the rig and engine nozzles, mainly by the different slopes of the hub walls and, also by the different cone angles of the jets (fig. 7). The influence of external flow, predictably, leads to the shift of the position of maxima to the downstream direction. It is important that for most harmonics the maxima of noise from engine nacelle is slightly higher than noise from the rig nozzle. The differences should be taken into account while estimating acoustic characteristics of the plane.

We should attract attention to the complex structure of computational curves. High precision experimental results [16] confirm the same behavior of experimental curves. So for further validation of the computational code it is very important to obtain experimental results with high resolution.

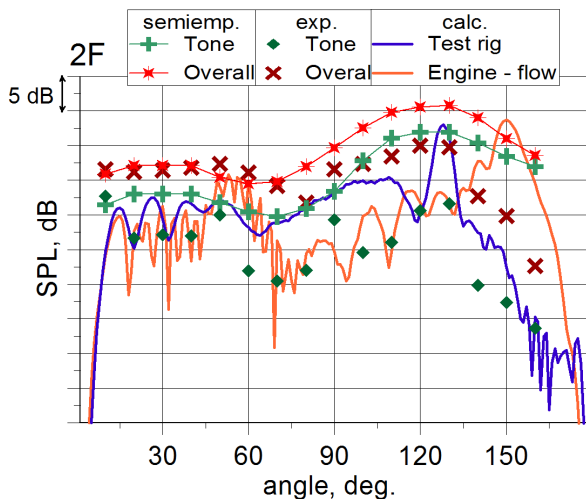


Fig. 10. Comparison between directivity diagrams for the second BPF harmonic at the distance 50 m. (engine scale)

In the last step of the work we compared the results of our calculation with the results of the semi-empirical calculation (based on the Heidmann model [17]). For this comparison we used data from the third set of microphones. In the fig. 10 are presented directivity diagrams for this set for the second BPF harmonic (we presented only results for the rig and for the engine nacelle in flow cases). Additionally in the plot are presented the results for this harmonic, obtained using semi-empirical model of fan tone noise. We see that this curve lays

higher than the computational curve. Moreover in the fig. 10 are presented the results of noise estimations for the overall (tone + broadband) noise of the fan in the 1/3-octave band containing this BPF tone. We see that for this 1/3-octave broadband noise dominates. The situation is the same for the other harmonics considered in the calculation. Also, as we can see, broadband contribution dominates in the experimental data too. So we can conclude that in order to perform computational estimation of the fan contribution to the flyover noise of airplane, we should have effective numerical method for broadband noise calculation.

7 Conclusions

An effort of aircraft flyover noise estimations with the usage of data, obtained in the 3D unsteady calculation of tone noise is presented. As input data we used the results of rotor - stator and rotor - IGV of booster interactions calculations performed with CIAM 3DAS aeroacoustic solver for the fan stage at approach conditions. These data were used for the calculation of noise radiation to the far field for three cases of fan mount. First case - the fan mounted in the test rig. Second case - the fan mounted in the engine nacelle in static conditions. Third case - the fan mounted in the engine nacelle in flight conditions.

The results of calculations (at rig scale) were compared with each other and with the experimental data. Comparison with the experiment showed satisfactory qualitative and in some positions of microphones quantitative agreement between the results of the simulation for rig inlet and nozzle and the experiment for the 2-nd, 3-rd and 4-th harmonics of BPF. Comparison between different cases of mount showed significant influence of external flow on the directivity diagram. The differences in directivity diagrams between rig mount and engine nacelle mount of fans are not so significant, but can not be neglected.

The results of computation in the far field were compared with the results of semi-empirical estimations of tone noise for specified harmonics and estimations of overall (tone + broadband) noise in the 1/3 octaves containing

these harmonics. It was found that in these 1/3 octaves broadband noise dominates over tone noise. In order to computationally estimate aircraft flyover noise at approach conditions the numerical method of broadband noise calculation should be used in pair with the method of tone noise calculation.

References

- [1] Nyukhtikov M., Brailko I., Milesin V., Pankov S. Computational and Experimental Investigation of Unsteady and Acoustic Characteristics of Counter – Rotating Fans. *ASME Heat Transfer / Fluids engineering Summer Conference*, Charlotte, North Carolina USA, HT-FED2004-56435, July 11-15, 2004.
- [2] Nyukhtikov M.A., Rossikhin A.A., Sgadlev V.V., Brailko I.A. Numerical Method for Turbo-Machinery Tonal Noise Generation and Radiation Simulation Using CAA Approach. *ASME Turbo Expo 2008*, Berlin, Germany, GT2008-51182, June 9-13, 2008.
- [3] Rossikhin A, Pankov S., Brailko I., Milesin V. Numerical Method For 3D Computation Of Turbomachinery Tone Noise. *International Conference Fan 2012*, Senlis, France, Paper 035, April 18-20, 2012.
- [4] Rossikhin A.A., Pankov S.V., Khaletskiy Y., Milesin V. Computational study on acoustic features of fan model with leaned stators. *ASME Turbo Expo 2014*, Düsseldorf, Germany, GT2014-26350, June 16-20, 2014.
- [5] Rossikhin A.A., Pankov S.V., Brailko I., Milesin V. Numerical investigation of high bypass ratio fan tone noise. *ASME Turbo Expo 2014*, Düsseldorf, Germany, GT2014-26354, June 16-20, 2014.
- [6] Milesin V., Khaletskiy Y., Shipov R. New acoustic facility for testing universal propulsion simulators, *Proceedings of the 13th International Congress on Sound and Vibration*, Wien, Paper # 142, 2006.
- [7] Nark D. M., Envia E., Burley C. L. Fan Noise Prediction with Applications to Aircraft System Noise Assessment. *15th AIAA/CEAS Aeroacoustics Conference*, Miami, Florida, AIAA-2009-3291, May 11-13, 2009.
- [8] Weckmüller C., Guerin S., Ashcroft G. CFD-CAA Coupling Applied to DLR UHBR-Fan: Comparison to Experimental Data. *15th AIAA/CEAS Aeroacoustics Conference*, Miami, Florida, AIAA 2009-3342, May 11-13, 2009.
- [9] Olausson M., Eriksson L.-E. RotorWake/Stator Broadband Noise Calculations Using Hybrid RANS/LES and Chorochronic Buffer Zones. *15th AIAA/CEAS Aeroacoustics Conference*, Miami, Florida, AIAA 2009-3338, May 11-13, 2009.
- [10] Tam C.K.W., Webb J.C. Dispersion-Relation-Preserving Schemes for Computational Acoustics. *Journal of Computational Physics*, Vol. 107, pp. 262-281, 1993.
- [11] Hu F.Q., Hussaini M.Y., Manthey J. Low-Dissipation and Low-Dispersion Runge-Kutta Schemes for Computational Acoustics. *Journal of Computational Physics*, Vol. 124, pp. 177-191, 1996.
- [12] Vasilyev O. A General Class of Commutative Filters for LES in Complex Geometries. *Journal of Computational Physics*, Vol. 146, pp. 82–104, 1998.
- [13] Zhang X., Chen X.X., Morfey C. L. and Tester B.J. Computation of fan noise radiation through a realistic engine exhaust geometry with flow. *9th AIAA/CEAS Aeroacoustics Conference*, Hilton Head, South Carolina, USA, AIAA 2003-3267, May 12-14, 2003.
- [14] Brentner K.S., Farassat F. Analytical Comparison of the Acoustic Analogy and Kirchhoff Formulation for Moving Surfaces, *AIAA Journal*, Vol. 36, No. 8, pp. 1379–1386, 1998.
- [15] Tyler J.M., Sofrin T.G. Axial Flow Compressor Noise Studies, *SAE Transactions*, Vol. 70, pp. 309–332, 1962.
- [16] Shah P. N., Vold H., Hensley D., Envia E., and Stephens D. A High-Resolution, Continuous-Scan Acoustic Measurement Method for Turbofan Engine Applications. *ASME Turbo Expo 2014*, Düsseldorf, Germany, GT2014-27108, June 16-20, 2014.
- [17] Heidmann M. F. – Interim prediction method for fan and compressor source noise, *NASA TM-X-71763*, 1979.

Copyright Statement

The authors confirm that they, and/or their company or organization, hold copyright on all of the original material included in this paper. The authors also confirm that they have obtained permission, from the copyright holder of any third party material included in this paper, to publish it as part of their paper. The authors confirm that they give permission, or have obtained permission from the copyright holder of this paper, for the publication and distribution of this paper as part of the ICAS 2014 proceedings or as individual off-prints from the proceedings.